SUPPLEMENTARY MATERIAL

Hydroxypyridinones with enhanced iron chelating properties. Synthesis, characterization and *in vivo* tests of 5-hydroxy-2-(hydroxymethyl)pyridine-4(1H)-one.

Joanna I. Lachowicz*[1], Valeria M. Nurchi[1], Guido Crisponi[1], Guadalupe Jaraquemada-Pelaez[1], Massimiliano Arca[1], Anna Pintus[1], Maria Amelia Santos[2], Catarina Quintanova[2], Lurdes Gano[3], Zbigniew Szewczuk[4], Maria Antonietta Zoroddu[5], Massimiliano Peana[5], Alicia Domínguez-Martín[6] and Duane Choquesillo-Lazarte[7]

[1]Dipartimento di Scienze Chimiche e Geologiche, Università di Cagliari, Cittadella Universitaria, 09042 Monserrato-Cagliari, Italy

[2]Centro Quimica Estrutural, Instituto Superior Tecnico, Universidade de Lisboa, Av. Rovisco Pais, 1049-001 Lisboa, Portugal.

[3]Campus Tecnológico e Nuclear, Instituto Superior Técnico, Universidade de Lisboa, Estrada Nacional 10, 2695-066 Bobadela LRS, Portugal

[4]Faculty of Chemistry, University of Wroclaw, F. Joliot-Curie 14, 50-383 Wroclaw, Poland

[5]Dipartimento di Chimica e Farmacia, Università di Sassari, Via Vienna 2, 07100 Sassari, Italy

[6]Department of Inorganic Chemistry, Faculty of Pharmacy, Campus Cartuja, University of Granada, E-18071, Granada, Spain

[7]Laboratorio de Estudios Cristalográficos, IACT, CSIC-Universidad de Granada, Av. de las Palmeras 4, E-18100 Armilla, Granada, Spain

Corresponding author

Joanna I. Lachowicz, Dipartimento di Scienze Chimiche e Geologiche, Cittadella Universitaria, 09042 Monserrato-Cagliari. Phone +39 070 675 4471 Fax +39 070 675 4478 email: lachowicz@unica.it

Table S1. Crystal data and structure refinement for P1.

Table S2. Atomic coordinates (x 10^4) and equivalent isotropic displacement parameters (A^2 x 10^3) for P1. U(eq) is defined as one third of the trace of the orthogonalized Uij tensor.

Table S3. Bond lengths [A] and angles [deg] for P1.

Table S4. Anisotropic displacement parameters (A^2 x 10^3) for P1. The anisotropic displacement factor exponent takes the form: -2 pi^2 [h^2 a*^2 U11 + ... + 2 h k a* b* U12]

Table S5. Hydrogen coordinates (x 10^4) and isotropic displacement parameters (A^2 x 10^3) for P1.

Table S6. Hydrogen bonds for P1 [A and deg.].

Table S7. Selected optimized bond lengths (Å) and angles (°) for the different forms of H_2L in the gas phase and in water (IEF-PCM SCRF model, in parenthesis).

Table S8. Selected optimized bond lengths (Å) and angles (°) for $Fe(P1^{-})_3$ and $[FeL_3]^{3-}$in the gas phase.

Figure S1. DFT optimized geometries of the three possible neutral forms of ligand H_2L in the gas phase, showing the different types of hydrogen bond-type interactions.

Table S9. Orthogonal Cartesian coordinates (Å) for the optimized structure of H_3L^{+} in the gas phase.

Table S10. Orthogonal Cartesian coordinates (Å) for the optimized structure of H_3L^{+} in water (IEF-PCM SCRF model).

Table S11. Orthogonal Cartesian coordinates (Å) for the optimized structure of H_2La in the gas phase.

Table S12. Orthogonal Cartesian coordinates (Å) for the optimized structure of H_2La in water (IEF-PCM SCRF model).

Table S13. Orthogonal Cartesian coordinates (Å) for the optimized structure of H_2Lb in the gas phase.

Table S14. Orthogonal Cartesian coordinates (Å) for the optimized structure of H_2Lb in water (IEF-PCM SCRF model).

Table S15. Orthogonal Cartesian coordinates (Å) for the optimized structure of H_2Lc in the gas phase.

Table S16. Orthogonal Cartesian coordinates (Å) for the optimized structure of H_2Lc in water (IEF-PCM SCRF model).

Table S17. Orthogonal Cartesian coordinates (Å) for the optimized structure of HLa^{-} in the gas phase.

Table S18. Orthogonal Cartesian coordinates (Å) for the optimized structure of HLa^{-} in water (IEF-PCM SCRF model).

Table S19. Orthogonal Cartesian coordinates (Å) for the optimized structure of HLb^{-} in the gas phase.

Table S20. Orthogonal Cartesian coordinates (Å) for the optimized structure of HLb^- in water (IEF-PCM SCRF model).

Table S21. Orthogonal Cartesian coordinates (Å) for the optimized structure of HLc^- in the gas phase.

Table S22. Orthogonal Cartesian coordinates (Å) for the optimized structure of HLc^- in water (IEF-PCM SCRF model).

Table S23. Orthogonal Cartesian coordinates (Å) for the optimized structure of L^{2-} in the gas phase.

Table S24. Orthogonal Cartesian coordinates (Å) for the optimized structure of L^{2-} in water (IEF-PCM SCRF model).

Table S25. Orthogonal Cartesian coordinates (Å) for the optimized structure of $Fe(HL^-)_3$ in the gas phase.

Table S26. Orthogonal Cartesian coordinates (Å) for the optimized structure of $[Fe(L^{2-})_3]^{3-}$ in the gas phase.

Figure S2A. UV spectra collected during potentiometric titration of the ligand, CL 4.95 x 10-4 M, using a 0.2 cm optical path length. A pH 2.98-4.59, B 7.29-10.52, C pH 10.64-13.22; D Absorptivity spectra of the ligand in the acidic and basic forms. 200-340 nm spectral range.

Figure S2B. UV spectra collected during potentiometric titration of the ligand, CL 4.95 x 10-4 M, using a 0.2 cm optical path length. A pH 2.98-4.59, B 7.29-10.52, C pH 10.64-13.22. 240-340 nm spectral range.

Figure S3. Absorptivity spectra of Fe^{3+}-P1 complexes calculated by HypSpec program using the data at 25˚C, 0.1 M KCl ionic strength, CL 4.9 × 10-4 M, 1:3 Fe/L molar ratio, optical path length 1 cm. The spectra are divided in A and B parts for clarity.

Figure S4. Stacked 1D ^1H NMR spectra in the aromatic region for P1 ligand by changing the pH from 0.65 to 13.30, at 298 K.

Table S27. Chemical shifts assignment for ^1H of P1 by changing the pH from 0.65 to 13.30, in aqueous solution (90%-10% H_2O-D_2O), at 298 K.

Figure S5. Superimposition of 2D ^1H-^{13}C spectra for the free P1 ligand at different pH values. In the inset a plot of the relative ^{13}C chemical shift variation $\Delta\delta=\delta_{pHi}-\delta_{pH0}$ for C6 (●), C3 (■) and C7 (▲); pH_0=1.67 (red), and pH_i=5.7 (orange), 8.2 (green) and 12.4 (blue), respectively.

Figure S6. Stacked aromatic region of 1D ^1H NMR spectra of the P1 ligand by increasing of substoichiometric amounts of Fe^{3+} ion, in phosphate buffer solution (pH = 7) at 298 K. In the inset, the relative ratio of H3/H6 in term of peak integral (black rhombus) and peak height (orange square).

Figure S7. Stacked 1D ^{1}H NMR spectra of P1 ligand by increasing amount of Ga^{3+}, as a diamagnetic probe of Fe^{3+}, in phosphate buffer solution at 298 K.

Figure S8. The comparison of the relative ratio of H3/H6 in term of peak integral and peak high ratio between pH 7 (black square) and pH 11,5 (orange rhombus)

Figure S9. Experimental data for peaks of the P1 ligand at pD 7 in D_2O solution are shown at the top of the panel and compared with the data calculated for the $[C_6H_8O_3N]^+$ (142.061 m/z, Panel A) $[C_6H_7DO_3N]^+$ (143.057 m/z, Panel B), $[C_6H_6D_2O_3N]^+$ (144.063 *m/z,* Panel C), $[C_6H_5D_3O_3N]^+$ (145.070 *m/z*, Panel D) and $[C_6H_4D_4O_3N]^+$ (146.076 *m/z* Panel E).

Table S28. ESI-MS *m/z* data of water ligand solution in different pH.

Figure S10. Fe^{3}+–P1 complexes. Experimental data for peak *m/z* = 333.998 (Panel A), 336.004 (Panel B), 409.940 (Panel C), 499.029 (Panel D) and 515.010 (Panel E) are shown at the top of the panel and compared with the data calculated for the Fe^{3+} complex (lower panel).

Table S29. ESI-MS *m/z* data of water Fe^{3+} – P1 solution in different pH.

Figure S11. Al^{3+}–P1 complexes. Experimental data for peak *m/z* = 305.030 (Panel A), 307.056 (Panel B), 448.101 (Panel C), 470.074 (Panel D) and 486.048 (Panel E) are shown at the top of the panel and compared with the data calculated for the Al^{3+} complex (lower panel).

Table S30. ESI-MS *m/z* data of water Al^{3+} – P1 solution in different pH.

Figure S12. Cu^{2+}–P1 complexes. Experimental data for peak *m/z* = 236.924 (Panel A), 341.989 (Panel B), 344.009 (Panel C), 365.985 (Panel D) and 381.963 (Panel E) are shown at the top of the panel and compared with the data calculated for the Cu^{2+} complex (lower panel).

Table S31. ESI-MS *m/z* data of water Cu^{2+} – P1 solution in different pH.

Figure S13. Zn^{2+}–P1 complexes. Experimental data (pH 7.0) for peak *m/z* = 382.970 are shown at the top of the panel and compared with the data calculated for the Zn^{2+} complex (lower panel).

Table S32. Complex formation constants (log β) of P1 with Fe^{3+}, Al^{3+}, Cu^{2+} and Zn^{2+} ions, and literature complex formation constants of DFP and 3,4-hopo. The charges are omitted for simplicity.

Table S1. Crystal data and structure refinement for P1.

Identification code	15jnac842
Empirical formula	$C_6H_7NO_3$
Formula weight	141.13
Temperature	100(2) K
Wavelength	0.71073 Å
Crystal system, space group	Orthorhombic, $P2_12_12_1$
Unit cell dimensions	a = 6.8410(4) Å α = 90°
	b = 7.0291(3) Å β = 90°
	c = 12.6402(4) Å γ = 90°
Volume	607.82(5) $Å^3$
Z, Calculated density	4, 1.542 Mg/m^3
Absorption coefficient	0.125 mm^{-1}
F(000)	296
Crystal size	0.100 x 0.100 x 0.100 mm
Theta range for data collection	3.223° to 27.492°
Limiting indices	-8<=h<=8, -9<=k<=9, -14<=l<=16
Reflections collec./unique	8040/1390 [R(int) = 0.0245]
Completeness to theta = 25.242	99.9 %
Refinement method	Full-matrix least-squares on F^2
Data / restraints / parameters	1390 / 0 / 91
Goodness-of-fit on F^2	1.094
Final R indices [I>2sigma(I)]	R1 = 0.0264, wR2 = 0.0666
R indices (all data)	R1 = 0.0278, wR2 = 0.0675
Absolute structure parameter	-0.5(4)
Extinction coefficient	n/a
Largest diff. peak and hole	0.251 and -0.186 $e.Å^{-3}$

Table S2. Atomic coordinates (x 10^4) and equivalent isotropic displacement parameters (A^2 x 10^3) for P1. U(eq) is defined as one third of the trace of the orthogonalized Uij tensor.

	x	y	z	U(eq)
O(4)	2319(2)	3426(2)	905(1)	14(1)
O(5)	-631(2)	5333(2)	1984(1)	17(1)
O(8)	6709(2)	5063(2)	4919(1)	14(1)
N(1)	3097(2)	4973(2)	3974(1)	12(1)
C(2)	4580(2)	4100(2)	3469(1)	12(1)
C(3)	4383(2)	3610(2)	2424(1)	12(1)
C(4)	2614(2)	3936(2)	1871(1)	12(1)
C(5)	1104(2)	4909(2)	2445(1)	12(1)
C(6)	1388(2)	5405(2)	3476(1)	13(1)
C(7)	6392(2)	3691(2)	4113(1)	14(1)

Table S3. Bond lengths [A] and angles [deg] for P1.

O(4)-C(4)	1.2887(19)
O(5)-C(5)	1.3555(19)
O(5)-H(5A)	0.8400
O(8)-C(7)	1.4200(19)
O(8)-H(8A)	0.8400
N(1)-C(2)	1.347(2)
N(1)-C(6)	1.363(2)
N(1)-H(1A)	0.8801
C(2)-C(3)	1.372(2)
C(2)-C(7)	1.510(2)
C(3)-C(4)	1.416(2)
C(3)-H(3)	0.9500
C(4)-C(5)	1.435(2)
C(5)-C(6)	1.363(2)
C(6)-H(6)	0.9500
C(7)-H(7A)	0.9900
C(7)-H(7B)	0.9900

C(5)-O(5)-H(5A)	109.5
C(7)-O(8)-H(8A)	109.5
C(2)-N(1)-C(6)	121.93(14)
C(2)-N(1)-H(1A)	119.0
C(6)-N(1)-H(1A)	119.0
N(1)-C(2)-C(3)	119.81(15)
N(1)-C(2)-C(7)	116.69(14)
C(3)-C(2)-C(7)	123.50(15)
C(2)-C(3)-C(4)	121.22(15)
C(2)-C(3)-H(3)	119.4
C(4)-C(3)-H(3)	119.4
O(4)-C(4)-C(3)	123.79(15)
O(4)-C(4)-C(5)	119.91(15)
C(3)-C(4)-C(5)	116.29(14)
O(5)-C(5)-C(6)	118.62(14)
O(5)-C(5)-C(4)	121.21(14)
C(6)-C(5)-C(4)	120.17(14)
N(1)-C(6)-C(5)	120.46(15)
N(1)-C(6)-H(6)	119.8
C(5)-C(6)-H(6)	119.8
O(8)-C(7)-C(2)	112.54(13)
O(8)-C(7)-H(7A)	109.1
C(2)-C(7)-H(7A)	109.1
O(8)-C(7)-H(7B)	109.1
C(2)-C(7)-H(7B)	109.1
H(7A)-C(7)-H(7B)	107.8

Symmetry transformations used to generate equivalent atoms:

Table S4. Anisotropic displacement parameters (A^2 x 10^3) for P1. The anisotropic displacement factor exponent takes the form: -2 pi^2 [h^2 a*^2 U11 + ... + 2 h k a* b* U12]

	U11	U22	U33	U23	U13	U12
O(4)	18(1)	14(1)	10(1)	-1(1)	0(1)	2(1)
O(5)	14(1)	24(1)	13(1)	-5(1)	-3(1)	5(1)
O(8)	16(1)	15(1)	11(1)	0(1)	0(1)	-3(1)
N(1)	13(1)	13(1)	10(1)	0(1)	0(1)	-1(1)
C(2)	12(1)	10(1)	14(1)	2(1)	1(1)	0(1)
C(3)	13(1)	11(1)	14(1)	-1(1)	3(1)	1(1)
C(4)	15(1)	9(1)	11(1)	2(1)	2(1)	-1(1)
C(5)	12(1)	12(1)	14(1)	1(1)	0(1)	0(1)
C(6)	11(1)	14(1)	14(1)	-1(1)	2(1)	1(1)
C(7)	14(1)	14(1)	14(1)	-1(1)	-2(1)	2(1)

Table S5. Hydrogen coordinates (x 10^4) and isotropic displacement parameters (A^2 x 10^3) for P1.

	x	y	z	U(eq)
H(5A)	-597	5024	1343	26
H(8A)	6997	6113	4642	21
H(1A)	3237	5274	4646	14
H(3)	5453	3043	2064	15
H(6)	386	6057	3850	16
H(7A)	6268	2418	4440	17
H(7B)	7540	3667	3636	17

Table S6. Hydrogen bonds for P1 [A and deg.].

D-H...A	d(D-H)	d(H...A)	d(D...A)	<(DHA)
O(5)-H(5A)...O(4)	0.84	2.36	2.7806(16)	111.9
O(5)-H(5A)...O(8)#1	0.84	1.95	2.7270(16)	152.4
O(8)-H(8A)...O(4)#2	0.84	1.83	2.6674(16)	177.4
N(1)-H(1A)...O(4)#3	0.88	1.87	2.7029(17)	156.1
C(6)-H(6)...O(4)#4	0.95	2.51	3.399(2)	156.0

Symmetry transformations used to generate equivalent atoms:
#1 -x+1/2,-y+1,z-1/2 #2 -x+1,y+1/2,-z+1/2 #3 -x+1/2,-y+1,z+1/2
#4 -x,y+1/2,-z+1/2

	H_3L^+	H_2L_a	H_2L_b	H_2L_c	HL_a^-	HL_b^-	HL_c^-	L^{2-}
N1-H1	1.025 (1.023)	1.014 (1.017)	/	1.018 (1.021)	/	1.011 (1.015)	/	/
N1-C2	1.337 (1.336)	1.349 (1.344)	1.325 (1.327)	1.336 (1.332)	1.321 (1.322)	1.345 (1.337)	1.327 (1.328)	1.322 (1.322)
C2-C3	1.389 (1.388)	1.373 (1.378)	1.400 (1.399)	1.397 (1.397)	1.411 (1.410)	1.383 (1.384)	1.398 (1.398)	1.404 (1.404)
C3-C4	1.392 (1.391)	1.435 (1.428)	1.386 (1.388)	1.385 (1.383)	1.379 (1.379)	1.448 (1.347)	1.417 (1.416)	1.433 (1.425)
C4-O4	1.325 (1.324)	1.237 (1.294)	1.351 (1.342)	1.310 (1.319)	1.335 (1.337)	1.235 (1.248)	1.265 (1.269)	1.258 (1.266)
O4-H4	0.966 (0.967)	/	0.963 (0.965)	1.010 (1.005)	1.014 (1.004)	/	/	/
C4-C5	1.425 (1.423)	1.470 (1.463)	1.408 (1.412)	1.467 (1.459)	1.452 (1.448)	1.523 (1.509)	1.455 (1.451)	1.519 (1.502)
C5-O5	1.322 (1.331)	1.328 (1.336)	1.345 (1.345)	1.253 (1.266)	1.276 (1.280)	1.245 (1.262)	1.348 (1.349)	1.265 (1.275)
O5-H5	0.968 (0.969)	0.987 (0.987)	0.966 (0.968)	/	/	/	0.998 (0.992)	/
C5-C6	1.380 (1.377)	1.361 (1.362)	1.389 (1.387)	1.405 (1.406)	1.408 (1.407)	1.418 (1.407)	1.372 (1.373)	1.424 (1.415)
N1-C6	1.349 (1.348)	1.374 (1.368)	1.334 (1.337)	1.362 (1.361)	1.348 (1.349)	1.382 (1.377)	1.356 (1.355)	1.365 (1.363)
C2-C7	1.504 (1.501)	1.510 (1.512)	1.515 (1.515)	1.507 (1.510)	1.520 (1.518)	1.499 (1.508)	1.524 (1.521)	1.526 (1.522)
C7-O8	1.393 (1.395)	1.405 (1.402)	1.384 (1.393)	1.405 (1.402)	1.391 (1.396)	1.419 (1.408)	1.391 (1.395)	1.396 (1.398)
O8-H8	0.962 (0.962)	0.963 (0.965)	0.976 (0.979)	0.963 (0.964)	0.989 (0.985)	0.964 (0.964)	0.990 (0.986)	1.015 (0.995)
N1-C2-C3	118.70 (118.88)	120.74 (120.46)	122.05 (122.43)	118.96 (118.93)	122.50 (122.45)	118.96 (119.02)	124.46 (124.17)	123.00 (122.70)
C2-C3-C4	119.36 (119.25)	120.59 (120.53)	118.47 (118.40)	119.32 (118.16)	117.40 (117.35)	123.70 (123.01)	119.62 (119.63)	122.74 (122.36)
C3-C4-C5	120.06 (119.98)	115.39 (115.56)	119.33 (119.07)	122.64 (122.74)	121.69 (121.81)	116.05 (116.52)	114.35 (114.57)	114.67 (115.19)
C4-C5-C6	117.89 (118.14)	121.34 (121.39)	117.61 (117.92)	114.80 (114.93)	114.65 (114.69)	115.05 (115.48)	121.39 (121.37)	115.06 (115.44)
C5-C6-N1	119.60 (119.47)	119.06 (118.86)	122.75 (122.64)	119.79 (119.79)	123.11 (123.10)	123.66 (123.07)	122.07 (121.92)	126.90 (126.47)
C6-N1-C2	124.38 (124.28)	122.88 (123.19)	119.79 (119.53)	125.48 (125.45)	120.65 (120.89)	122.57 (122.87)	118.10 (118.34)	117.63 (117.82)
C2-N1-H1	114.54 (115.21)	116.31 (116.17)	/	114.86 (114.78)	/	117.52 (116.85)	/	/
C5-C4-O4	114.15 (114.39)	116.86 (116.78)	115.27 (116.18)	111.46 (111.77)	111.27 (111.95)	121.35 (120.32)	116.25 (116.57)	121.65 (120.90)
C4-O4-H4	113.71 (113.05)	/	110.80 (111.66)	99.48 (99.56)	96.88 (98.30)	/	/	/
C6-C5-O5	120.46 (120.81)	124.97 (124.76)	121.37 (121.21)	129.75 (129.40)	130.16 (129.53)	123.88 (124.24)	126.32 (125.61)	123.59 (123.72)
C5-O5-H5	110.47 (109.27)	101.60 (101.14)	108.06 (108.31)	/	/	/	98.03 (99.32)	/
N1-C2-C7	116.05 (116.40)	114.92 (115.32)	115.12 (114.74)	116.08 (116.34)	114.05 (114.41)	116.43 (116.37)	112.88 (113.35)	112.11 (113.35)
C2-C7-O8	106.79 (107.45)	112.33 (112.32)	111.38 (110.67)	112.03 (111.87)	109.99 (109.85)	112.85 (112.77)	110.28 (110.09)	109.06 (109.19)
C7-O8-H8	110.39 (110.07)	108.44 (108.65)	104.35 (103.39)	108.48 (108.76)	100.86 (101.58)	105.87 (108.12)	100.67 (101.42)	97.38 (99.70)
C3-C2-N1-H1	179.99	-177.57	/	-179.01	/	-178.10	/	/

	(180.00)	(-178.59)		(-179.61)		(-178.05)		
N1-C6-C5-O5	180.00	179.96	-180.00	-179.95	-180.00	179.73	-180.00	179.99
	(179.99)	(179.76)	(-180.00)	(-180.00)	(-179.96)	(179.31)	(-180.00)	(180.00)
C6-C5-O5-H5	179.99	179.50	-179.95	/	/	/	-180.00	-179.99
	(179.99)	(179.54)	(-179.99)				(-179.99)	(-179.99)
C6-C5-C4-O4	179.99	-179.41	179.99	-179.33	180.00	-179.24	-179.99	/
	(180.00)	(-179.57)	(180.00)	(-179.63)	(180.00)	(-178.72)	(-179.99)	
C5-C4-O4-H4	179.93	/	179.96	-0.12	0.00	/	/	179.99
	(179.99)		(179.99)	(-0.07)	(0.02)			(180.00)
C6-N1-C2-C7	179.98	-177.52	179.99	-177.2	-180.00	-177.46	179.99	/
	(179.99)	(-177.84)	(180.00)	-(177.92)	(-180.00)	(-176.93)	(179.99)	
N1-C2-C7-O8	0.04	-26.46	0.01	-23.02	-0.01	-40.82	-0.02	-0.05
	(0.07)	(-18.82)	(0.01)	(-13.34)	(0.01)	(-25.69)	(-0.02)	(0.00)
C2-C7-O8-H8	-179.91	-77.01	-0.01	-78.8	0.00	-49.15	0.02	0.03
	(-179.87)	(-81.76)	(-0.01)	(-86.29)	(0.00)	(-71.82)	(0.01)	(0.02)

Table S7. Selected optimized bond lengths (Å) and angles (°) for the differently protonated forms of **P1**[a] in the gas phase and in water (IEF-PCM SCRF model, in parenthesis).[b]

[a] The neutral form of **P1** corresponds to H_2L. [b]Atom numbering scheme as in Figure 1. Molecular schemes as in Scheme 2.

Table S8. Selected optimized bond lengths (Å) and angles (°) for Fe^{3+}–**P1**[a] complexes in the gas phase.[b]

	$Fe(HL)_3$	$[Fe(L)_3]^{3-}$		$Fe(HL)_3$	$[FeL_3]^{3-}$
Fe-O4	2.082	2.082	O5-Fe-O20	96.43	98.15
Fe-O5	1.994	2.030	O4-C4-C5	116.58	116.71
Fe-O12	2.082	2.081	O5-C5-C4	116.35	114.78
Fe-O13	1.995	2.030	C2-N1-H1	116.02	/
Fe-O20	2.081	2.081	C3-C2-C7	124.64	123.79
Fe-O21	1.995	2.030	C2-C7-O8	112.30	109.61
C4-O4	1.263	1.280	C7-O8-H8	108.22	99.08
C5-05	1.287	1.295	O12-C12-C13	116.56	116.71
C12-O12	1.263	1.280	O13-C13-C12	116.34	116.36
C13-O13	1.287	1.295	C10-N9-H9	115.97	/
C20-O20	1.263	1.280	C11-C10-C15	124.60	123.82
C21-O21	1.287	1.295	C10-C15-O16	112.33	109.60
N1-C2	1.343	1.324	C15-O16-H16	108.26	99.08
N1-C6	1.368	1.356	O20-C20-C21	116.58	116.72
N1-H1	1.015	/	O21-C21-C20	116.34	116.35
C4-C5	1.466	1.459	C18-N17-H17	116.02	/
C2-C7	1.508	1.525	C19-C18-C23	124.60	123.79
C7-O8	1.406	1.394	C18-C23-O24	112.33	109.60
O8-H8	0.963	1.000	C23-O24-H24	108.25	99.08
N9-C10	1.343	1.324	Fe-O4-C4-C3	-178.62	-179.71
N9-C14	1.368	1.356	Fe-O5-C5-C6	177.91	179.45
N9-H9	1.015	/	Fe-O12-C12-C11	-179.17	-179.57
C12-C13	1.466	1.459	Fe-O13-C13-C14	178.55	179.27
C10-C15	1.508	1.525	Fe-O20-C20-C19	-178.87	-179.67
C15-O16	1.406	1.394	Fe-O21-C21-C22	178.19	179.35
O16-H16	0.963	1.000	O4-Fe-O13-C13	88.74	91.93
N17-C18	1.343	1.324	O12-Fe-O21-C21	89.12	92.08
N17-C22	1.368	1.356	O20-Fe-O5-C5	89.47	91.86
N17-H17	1.015	/	O4-C4-C5-O5	0.39	0.02
C21-C20	1.466	1.459	C3-C2-N1-H1	-178.09	/
C18-C23	1.508	1.525	C6-N1-C2-C7	-177.55	-179.95
C23-O23	1.406	1.394	N1-C2-C7-O8	-26.57	0.19
O23-H23	0.963	1.000	C2-C7-O8-H8	-74.65	-0.01
Fe-O5-C5	114.96	114.78	O12-C12-C13-O13	0.35	0.28
Fe-O4-C4	112.80	113.37	C11-C10-N9-H9	-178.22	/
O4-Fe-O5	79.29	78.77	C14-N9-C10-C15	-177.46	-179.95
O4-Fe-O13	96.15	98.15	N9-C10-C15-O16	-26.15	0.02
Fe-O12-C12	112.84	113.38	C10-C15-O16-H16	-75.07	0.00
Fe-O13-C13	114.96	114.75	O20-C20-C21-O21	0.38	0.30
O12-Fe-O13	79.29	78.77	C19-C18-N17-H17	-178.14	/
O12-Fe-O21	96.48	98.16	C22-N17-C18-C23	-177.52	-179.99
Fe-O20-C20	112.83	113.39	N17-C18-C23-O24	-26.37	-0.05
Fe-O21-C21	114.94	114.76	C18-C23-O24-H24	-74.83	0.08

O20-Fe-O21	79.30	78.78

[a] The neutral form of **P1** corresponds to H_2L. [b] Atom numbering scheme as in Figure 1. Molecular schemes as in Scheme 2.

Figure S1. DFT optimized geometries of the three possible neutral forms of ligand **P1** in the gas phase, showing the different types of hydrogen bond-type interactions.

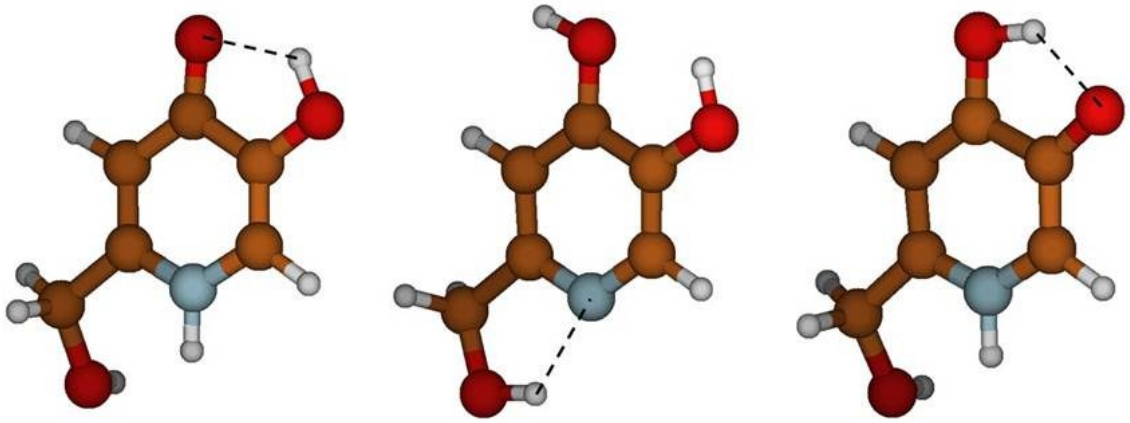

H_2L_a H_2L_b H_2L_c

Table S9. Orthogonal Cartesian coordinates (Å) for the optimized structure of the fully protonated form of **P1** (H_3L^+ in Scheme 2) in the gas phase.

	x	y	z
C	2.945804	2.484780	3.025241
C	3.155706	2.988988	4.302337
N	2.177772	3.689788	4.884605
C	0.982505	3.948037	4.314960
C	0.714974	3.473394	3.047240
C	1.730106	2.721034	2.389296
C	4.413373	2.813613	5.109198
O	4.208281	3.468024	6.321339
O	-0.451170	3.716465	2.472635
O	1.395124	2.302246	1.178043
H	2.400707	4.031404	5.825342
H	0.255637	4.530354	4.879128
H	-0.483310	3.318720	1.590266
H	3.731065	1.909987	2.531742
H	4.601191	1.730995	5.232428
H	5.259444	3.231779	4.533231
H	4.979432	3.397963	6.892861
H	2.088285	1.793655	0.737242

Table S10. Orthogonal Cartesian coordinates (Å) for the optimized structure of the fully protonated form of **P1** (H_3L^+ in Scheme 2) in water (IEF-PCM SCRF model).

	x	y	z
C	2.942395	2.488697	3.031069
C	3.147308	2.994431	4.307009
N	2.169403	3.694803	4.888155
C	0.975624	3.951525	4.316038
C	0.714493	3.475357	3.050538
C	1.728600	2.723769	2.393703
C	4.405546	2.815396	5.105757
O	4.221677	3.464369	6.326916
O	-0.454400	3.712873	2.460704
O	1.399230	2.302838	1.182487
H	2.380188	4.040903	5.827673
H	0.253217	4.533674	4.884119
H	-0.458090	3.304419	1.582039
H	3.727846	1.914712	2.539865
H	4.591675	1.732943	5.221907
H	5.247538	3.231251	4.524423
H	5.010668	3.374596	6.870783
H	2.102011	1.794671	0.753951

Table S11. Orthogonal Cartesian coordinates (Å) for the optimized structure of $\mathbf{H_2L_a}$ (see Fig. S1; H_2L_a in Scheme 2) in the gas phase.

	x	y	z
C	3.123953	2.906948	4.350787
N	2.123778	3.524471	5.012545
H	2.320586	3.800797	5.968478
C	0.916561	3.823394	4.429139
H	0.175463	4.334822	5.040884
C	0.704490	3.472523	3.131366
O	-0.414590	3.702578	2.453617
H	-0.192850	3.322969	1.569387
C	1.744758	2.796246	2.342247
O	1.467464	2.525087	1.167093
C	2.973524	2.538551	3.036595
H	3.786924	2.045994	2.503522
C	4.350187	2.613362	5.181201
H	4.250787	1.610110	5.625290
H	5.237109	2.585434	4.527350
O	4.493283	3.506459	6.255999
H	4.832272	4.341155	5.915501

Table S12. Orthogonal Cartesian coordinates (Å) for the optimized structure of $\mathbf{H_2L_a}$ (see Fig. S1; H_2L_a in Scheme 2) in water (IEF-PCM SCRF model).

	x	y	z
C	3.125529	2.912598	4.343149
N	2.139466	3.555122	4.991772
H	2.341985	3.839968	5.946940
C	0.934779	3.853601	4.416218
H	0.208487	4.387514	5.026324
C	0.710288	3.475402	3.126818
O	-0.418770	3.706032	2.451060
H	-0.207610	3.303713	1.575032
C	1.730975	2.770717	2.350581
O	1.436859	2.472276	1.173921
C	2.957006	2.513236	3.035230
H	3.764927	1.998853	2.513961
C	4.362484	2.629476	5.164589
H	4.316554	1.584973	5.510959
H	5.252986	2.713511	4.522432
O	4.439109	3.437641	6.307425
H	4.798648	4.296267	6.054589

Table S13. Orthogonal Cartesian coordinates (Å) for the optimized structure of $\mathbf{H_2L_b}$ (see Fig. S1; H_2L_b in Scheme 2) in the gas phase.

	x	y	z
C	2.980648	2.452455	3.043749
C	3.217591	2.971846	4.321801
N	2.324094	3.719346	4.954007
C	1.157467	3.995089	4.368762
C	0.822977	3.529662	3.103992
C	1.770230	2.734975	2.429325
C	4.504314	2.725347	5.083038
O	4.486319	3.347501	6.318930
O	-0.361590	3.824827	2.540154
O	1.396296	2.307705	1.203297
H	0.439894	4.613940	4.914104
H	-0.391650	3.406539	1.670187
H	3.731570	1.837969	2.540224
H	4.646426	1.630772	5.186971
H	5.351879	3.084660	4.465283
H	3.616436	3.787831	6.355366
H	2.088669	1.772990	0.801731

Table S14. Orthogonal Cartesian coordinates (Å) for the optimized structure of $\mathbf{H_2L_b}$ (see Fig. S1; H_2L_b in Scheme 2) in water (IEF-PCM SCRF model).

	x	y	z
C	2.985379	2.449223	3.041801
C	3.220695	2.968924	4.318799
N	2.330915	3.717726	4.957384
C	1.161341	3.994741	4.371987
C	0.828281	3.529070	3.108226
C	1.773694	2.732038	2.426901
C	4.506745	2.723369	5.081373
O	4.471313	3.356173	6.321806
O	-0.357060	3.825485	2.546424
O	1.394835	2.311649	1.209713
H	0.444625	4.613871	4.918575
H	-0.392460	3.409171	1.673588
H	3.733958	1.835354	2.537029
H	4.652386	1.631832	5.193238
H	5.357335	3.084719	4.472187
H	3.592369	3.787489	6.331289
H	2.077221	1.772617	0.790602

Table S15. Orthogonal Cartesian coordinates (Å) for the optimized structure of $\mathbf{H_2L_c}$ (see Fig. S1; H_2L_c in Scheme 2) in the gas phase.

	x	y	z
C	4.347382	2.707331	4.991379
C	3.149003	2.903439	4.326192
C	2.103190	3.523212	5.013967
N	2.295290	3.898536	6.281614
C	3.444144	3.725117	6.991904
C	4.556185	3.119285	6.383482
C	0.766996	3.877309	4.413283
O	-0.218340	4.069259	5.396172
O	5.689854	2.869534	6.854542
O	5.417730	2.139169	4.494104
H	1.487606	4.329365	6.727535
H	3.450702	4.066268	8.024825
H	3.021285	2.581069	3.292546
H	0.847144	4.831541	3.867034
H	0.483858	3.113492	3.669538
H	-0.524610	3.205843	5.694143
H	6.026543	2.199638	5.297402

Table S16. Orthogonal Cartesian coordinates (Å) for the optimized structure of $\mathbf{H_2L_c}$ (see Fig. S1; H_2L_c in Scheme 2) in water (IEF-PCM SCRF model).

	x	y	z
C	4.361696	2.733701	4.987612
C	3.167792	2.928119	4.316753
C	2.107146	3.51183	5.013925
N	2.284858	3.854249	6.288933
C	3.431962	3.680682	7.000195
C	4.551728	3.108275	6.385286
C	0.762781	3.843166	4.412529
O	-0.176760	4.190735	5.393472
O	5.696923	2.864856	6.867676
O	5.449804	2.195017	4.473273
H	1.467823	4.269242	6.738354
H	3.420433	4.000656	8.040112
H	3.050215	2.634934	3.273375
H	0.878827	4.713167	3.746365
H	0.426754	3.005112	3.781527
H	-0.591560	3.385524	5.724781
H	6.053539	2.240141	5.275495

Table S17. Orthogonal Cartesian coordinates (Å) for the optimized structure of $\mathbf{HL_a^-}$ (HL_a^- in Scheme 2) in the gas phase.

	x	y	z
C	4.335389	2.746421	4.963361
C	3.162948	2.952067	4.266723
C	2.056879	3.447090	4.989083
N	2.114448	3.711622	6.281759
C	3.254920	3.514698	6.973696
C	4.437137	3.025619	6.385173
C	0.700764	3.723565	4.360005
O	-0.181200	4.202397	5.322789
O	5.578790	2.790618	6.904642
O	5.490728	2.287663	4.476031
H	3.243661	3.751468	8.043086
H	3.098514	2.738105	3.196031
H	0.818177	4.451760	3.527884
H	0.312542	2.793968	3.889251
H	0.398415	4.200170	6.123879
H	6.010686	2.319040	5.346359

Table S18. Orthogonal Cartesian coordinates (Å) for the optimized structure of $\mathbf{HL_a^-}$ (HL_a^- in Scheme 2) in water (IEF-PCM SCRF model).

	x	y	z
C	4.333738	2.748592	4.970871
C	3.162138	2.953356	4.271912
C	2.056044	3.448016	4.992402
N	2.113343	3.712909	6.286568
C	3.254950	3.515502	6.977868
C	4.435452	3.026943	6.388580
C	0.705137	3.721069	4.355177
O	-0.184020	4.202420	5.317318
O	5.576443	2.794391	6.921275
O	5.484155	2.288133	4.467961
H	3.243121	3.752220	8.047643
H	3.095986	2.740137	3.202132
H	0.825791	4.447665	3.526419
H	0.320649	2.792026	3.887860
H	0.381144	4.206295	6.124498
H	6.028726	2.306595	5.311267

Table S19. Orthogonal Cartesian coordinates (Å) for the optimized structure of $\mathbf{HL_b^-}$ (HL_b^- in Scheme 2)in the gas phase.

	x	y	z
C	3.091647	2.889898	4.390210
C	2.070692	3.570642	5.028158
N	2.264842	4.006700	6.285953
C	3.443011	3.790744	6.974575
C	4.563087	3.117546	6.424137
C	4.376378	2.613969	4.998923
C	0.763116	3.931875	4.391239
O	-0.333880	3.821395	5.284350
O	5.628199	2.924894	7.039155
O	5.272636	1.999803	4.411949
H	1.494207	4.475626	6.741912
H	3.478374	4.164331	7.999217
H	2.940450	2.527956	3.369166
H	0.750037	4.984635	4.055933
H	0.626219	3.308806	3.488595
H	-0.251270	2.954076	5.697425

Table S20. Orthogonal Cartesian coordinates (Å) for the optimized structure of $\mathbf{HL_b^-}$ (HL_b^- in Scheme 2) in water (IEF-PCM SCRF model).

	x	y	z
C	3.132426	2.915814	4.373972
C	2.086782	3.538335	5.033584
N	2.259790	3.928951	6.300537
C	3.437781	3.737545	6.987344
C	4.571584	3.133188	6.413644
C	4.408529	2.670097	4.986284
C	0.762831	3.884943	4.400846
O	-0.269410	4.036392	5.345588
O	5.665483	2.958083	7.018268
O	5.349838	2.100356	4.397304
H	1.462389	4.354165	6.761939
H	3.448892	4.084253	8.021466
H	2.991479	2.588191	3.340297
H	0.842915	4.854807	3.882701
H	0.519913	3.134926	3.629417
H	-0.493480	3.162852	5.687704

Table S21. Orthogonal Cartesian coordinates (Å) for the optimized structure of $\mathbf{HL_c^-}$ (HL_c^- in Scheme 2) in the gas phase.

	x	y	z
C	3.181835	3.051542	4.377208
C	2.079513	3.735221	4.947230
C	2.061665	3.992902	6.320868
N	3.023143	3.638658	7.163666
C	4.099644	2.981415	6.665020
C	4.215560	2.679300	5.331379
C	0.912202	4.722122	7.00588
O	1.159073	4.837735	8.369562
O	5.242653	2.032296	4.745793
O	3.388265	2.724907	3.172966
H	4.887179	2.694003	7.370442
H	1.254181	4.053833	4.304301
H	0.782503	5.719118	6.534125
H	-0.033090	4.172071	6.812866
H	2.037836	4.387004	8.435640
H	4.898965	2.044115	3.809091

Table S22. Orthogonal Cartesian coordinates (Å) for the optimized structure of $\mathbf{HL_c^-}$ (HL_c^- in Scheme 2) in water (IEF-PCM SCRF model).

	x	y	z
C	3.178371	3.053487	4.378714
C	2.077136	3.736605	4.948377
C	2.059295	3.994255	6.322387
N	3.025206	3.636961	7.160920
C	4.100640	2.980200	6.661379
C	4.212335	2.680011	5.325896
C	0.909813	4.722754	7.002111
O	1.157952	4.838777	8.370301
O	5.245644	2.031634	4.750433
O	3.375122	2.731258	3.167349
H	4.889385	2.691710	7.364362
H	1.249312	4.057479	4.310228
H	0.781136	5.718386	6.533165
H	-0.033350	4.173188	6.811957
H	2.033670	4.391480	8.448543
H	4.929464	2.028056	3.809917

Table S23. Orthogonal Cartesian coordinates (Å) for the optimized structure of $\mathbf{L_2^-}$ (L_2^- in Scheme 2) in the gas phase.

	x	y	z
C	3.160998	3.057819	4.325832
C	2.067758	3.744075	4.949269
C	2.028539	4.017242	6.326342
N	2.99379	3.664858	7.157968
C	4.070012	3.006162	6.636363
C	4.275301	2.648628	5.272944
C	0.891814	4.742628	7.040081
O	1.192248	4.833516	8.400883
O	5.301205	2.035773	4.856634
O	3.214359	2.803731	3.094564
H	4.867016	2.718759	7.341925
H	1.239486	4.05723	4.294949
H	0.734695	5.756314	6.594927
H	-0.07625	4.207141	6.877251
H	2.088426	4.358977	8.368409

Table S24. Orthogonal Cartesian coordinates (Å) for the optimized structure of $\mathbf{L_2^-}$ (L_2^- in Scheme 2) in water (IEF-PCM SCRF model).

	x	y	z
C	3.158920	3.061809	4.339810
C	2.069989	3.744349	4.956507
C	2.035595	4.014579	6.333393
N	3.006849	3.657191	7.155932
C	4.077905	3.000165	6.628146
C	4.265583	2.652953	5.268897
C	0.892080	4.740219	7.029030
O	1.175409	4.842118	8.394619
O	5.291962	2.035860	4.831092
O	3.220066	2.802842	3.102106
H	4.874849	2.711860	7.330133
H	1.238324	4.061521	4.313395
H	0.745969	5.744497	6.577439
H	-0.062880	4.198447	6.860608
H	2.058783	4.384440	8.417234

Table S25. Orthogonal Cartesian coordinates (Å) for the optimized structure of $Fe(HL)_3$ in the gas phase (**P1** = H_2L).

	x	y	z
C	-16.0987	4.753250	15.02005
C	-14.7985	4.966846	15.44034
C	-13.8956	5.694723	14.54406
C	-14.4048	6.148153	13.30176
C	-15.7200	5.904414	12.96012
N	-16.5157	5.231585	13.80765
O	-14.2970	4.569373	16.55690
Fe	-12.3653	4.996082	16.81116
O	-12.7096	5.857226	14.94661
C	-16.3836	6.397757	11.69918
O	-17.4894	5.609861	11.33499
O	-10.3403	5.434302	16.60824
C	-9.66733	4.454983	16.18048
C	-10.4086	3.220514	15.90478
C	-9.69809	2.122734	15.45444
N	-8.34653	2.212538	15.26029
C	-7.63305	3.324892	15.49903
C	-8.26714	4.460199	15.96254
O	-11.6771	3.256191	16.11906
C	-6.16486	3.239828	15.16547
O	-5.67909	1.921996	15.22518
O	-12.6524	6.857884	17.69643
C	-12.6662	6.803601	18.95802
C	-12.4709	5.481348	19.55974
C	-12.5014	5.383995	20.93897
N	-12.6911	6.503845	21.70224
C	-12.8712	7.731750	21.18897
C	-12.8658	7.910483	19.82005
O	-12.2962	4.502370	18.74272
C	-13.0053	8.844941	22.19729
O	-13.5012	8.390649	23.43170
H	-7.70057	5.368874	16.16723
H	-7.81811	1.403885	14.94786
H	-10.1729	1.165966	15.24589
H	-5.60188	3.931143	15.81440
H	-6.00430	3.577886	14.12909

H	-5.58902	1.675195	16.15205
H	-13.0169	8.900225	19.38861
H	-12.7347	6.433306	22.71411
H	-12.3838	4.435542	21.45947
H	-13.6144	9.656902	21.76635
H	-12.0113	9.272142	22.40631
H	-14.4445	8.220928	23.33389
H	-13.7450	6.687424	12.62175
H	-17.4631	5.058187	13.48648
H	-16.8229	4.205368	15.61976
H	-15.6318	6.474034	10.89605
H	-16.7746	7.414660	11.86408
H	-17.1614	4.781082	10.96941

Table S26. Orthogonal Cartesian coordinates (Å) for the optimized structure of $[Fe(L)_3]^{3-}$ in the gas phase (**P1** = H_2L).

	x	y	z
C	-16.1805	4.764977	15.08601
C	-14.8495	4.945252	15.51206
C	-13.9627	5.693586	14.64213
C	-14.4871	6.187603	13.44706
N	-15.7745	5.999243	13.06377
C	-16.5916	5.310046	13.85965
O	-14.3359	4.498936	16.62504
Fe	-12.3529	5.020929	16.86001
O	-12.7254	5.844765	15.05457
C	-18.0094	5.164817	13.32320
O	-18.1239	5.801492	12.08697
O	-12.6250	6.767131	17.83693
C	-12.6720	6.643861	19.14240
C	-12.8279	7.689024	20.05495
N	-12.8749	7.508805	21.39151
C	-12.7678	6.288831	21.87179
C	-12.6069	5.154047	21.06698
C	-12.5526	5.302534	19.67196
O	-12.4043	4.343790	18.80917
C	-12.8361	6.231146	23.38424
O	-12.9961	7.521469	23.89502
O	-11.7743	3.147818	16.21624
C	-10.4916	3.053134	16.01891
C	-9.70405	4.242956	16.28263
C	-8.32601	4.172192	16.07447
N	-7.69447	3.050835	15.64153
C	-8.41771	1.950954	15.39888
C	-9.81027	1.904173	15.57307
O	-10.3599	5.300908	16.70106
C	-7.60462	0.754403	14.91620
O	-6.25212	1.085701	14.84279
H	-10.3708	0.988382	15.36544
H	-7.70934	5.058538	16.26561
H	-7.98599	0.426073	13.92852
H	-7.76666	-0.100720	15.60259
H	-6.26835	2.028431	15.13821

H	-16.8793	4.204864	15.71357
H	-13.8378	6.758004	12.77242
H	-18.7252	5.589004	14.05560
H	-18.2625	4.088722	13.24132
H	-17.2084	6.149667	11.96239
H	-12.5220	4.157881	21.51022
H	-12.9201	8.715660	19.68228
H	-11.9160	5.755067	23.77800
H	-13.6723	5.571691	23.69155
H	-13.0138	8.058488	23.07061

Figure S2A. UV spectra collected during potentiometric titration of the ligand, C_L 4.95 x 10^{-4} M, using a 0.2 cm optical path length. A pH 2.98-4.59, B 7.29-10.52, C pH 10.64-13.22; D Absorptivity spectra of the ligand in the acidic and basic forms. 200-340 nm spectral range.

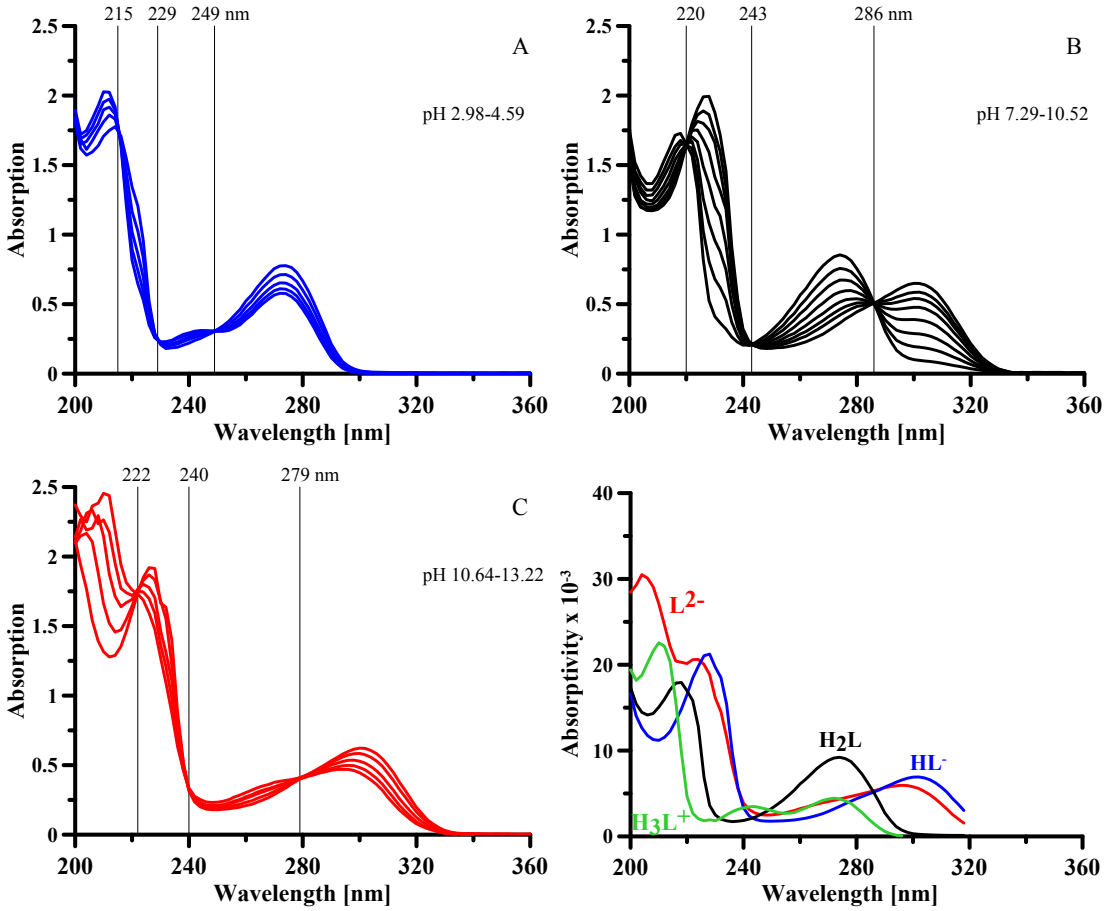

Figure S2B. UV spectra collected during potentiometric titration of the ligand, C_L 4.95 x 10^{-4} M, using a 0.2 cm optical path length. A pH 2.98-4.59, B 7.29-10.52, C pH 10.64-13.22. 240-340 nm spectral range.

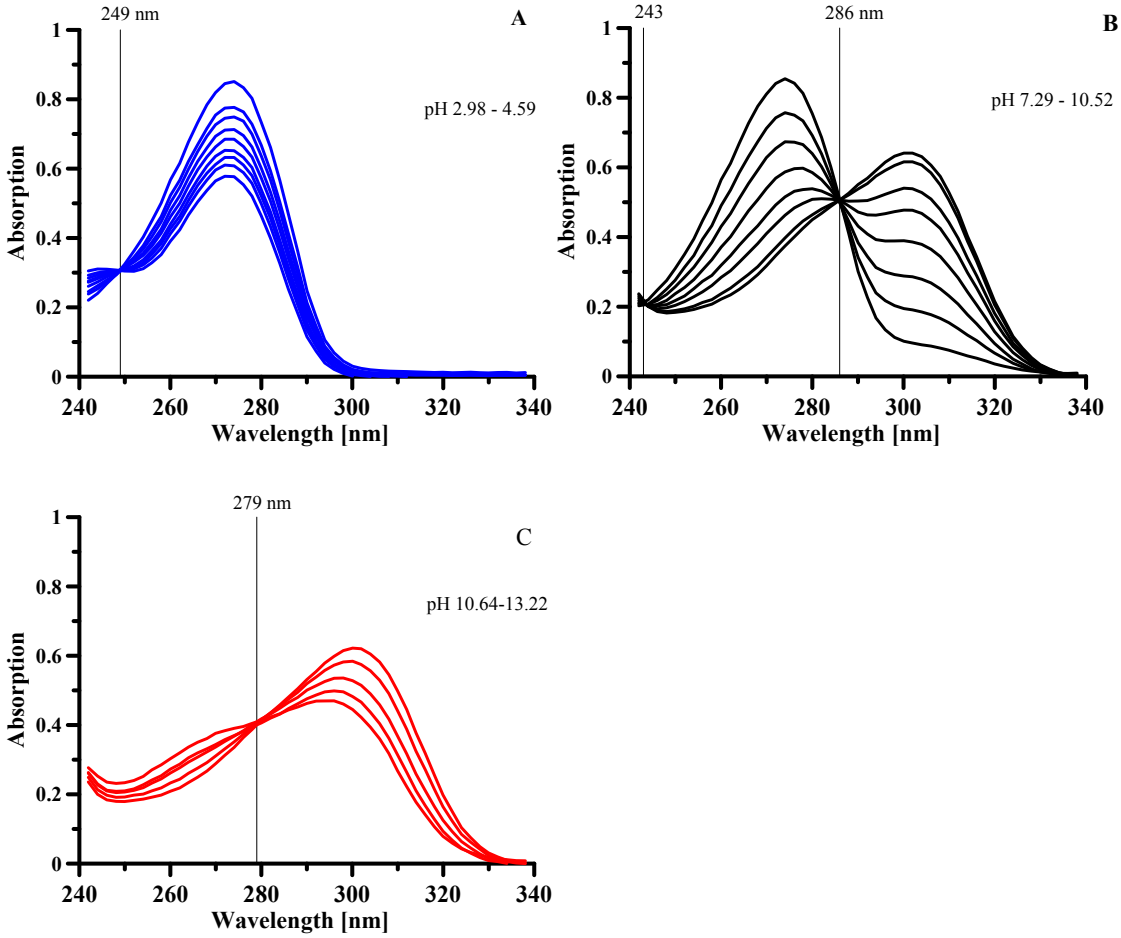

Figure S3. Absorptivity spectra of Fe^{3+}-P1 complexes calculated by HypSpec program using the data at 25˚C, 0.1 M KCl ionic strength, C_L 4.9 × 10^{-4} M, 1:3 Fe/L molar ratio, optical path length 1 cm. The spectra are divided in A,B and C parts for clarity.

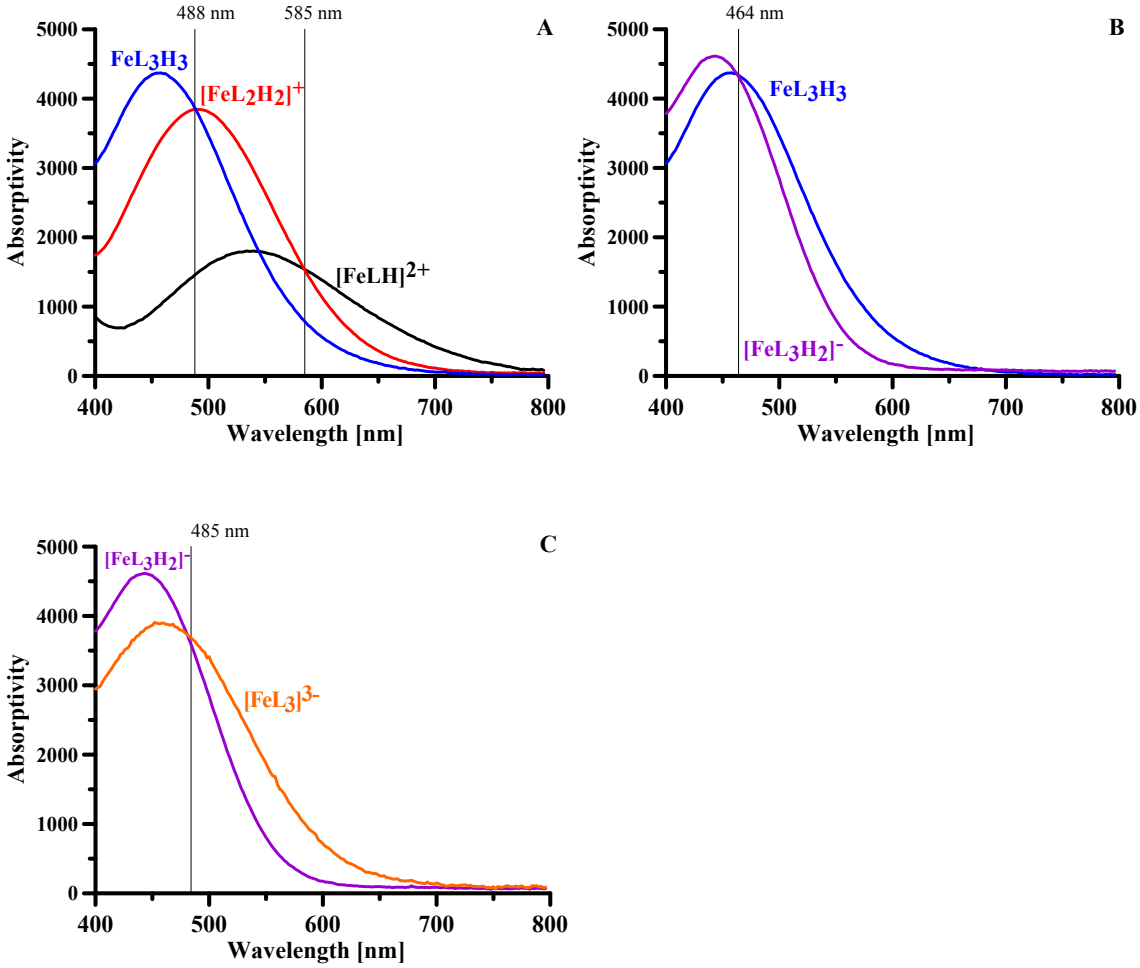

Figure S4. Stacked 1D ^{1}H NMR spectra in the aromatic region for P1 ligand by changing the pH from 0.65 to 13.30, at 298 K.

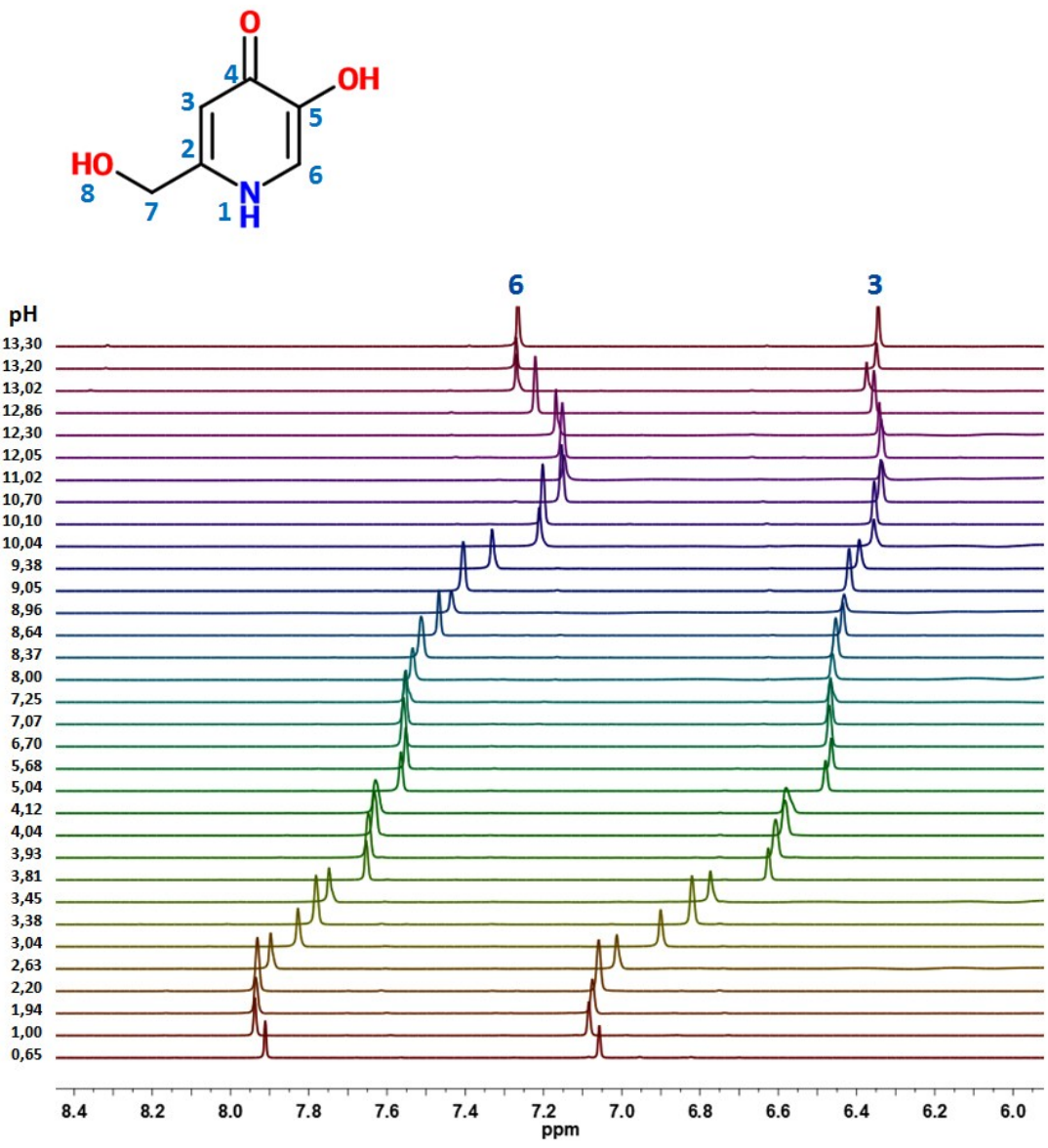

Table S27. Chemical shifts assignment for ^{1}H of P1 by changing the pH from 0.65 to 13.30, in aqueous solution (90%-10% H_2O-D_2O), at 298 K.

pH	H6	H3	H7
0.65	7.911	7.032	NA
1.00	7.938	7.084	NA
1.67	7.949	7.082	4.723
1.94	7.935	7.075	NA
2.20	7.931	7.059	NA
2.63	7.898	7.013	NA
3.04	7.828	6.901	NA
3.26	7.781	6.820	NA
3.45	7.731	6.738	4.624
3.38	7.748	6.774	NA
3.81	7.653	6.626	4.585
3.93	7.648	6.607	4.580
4.04	7.632	6.583	4.580
4.12	7.630	6.580	4.577
5.04	7.564	6.479	4.545
5.68	7.552	6.465	4.537
5.96	7.563	6.474	4.547
6.70	7.558	6.469	4.545
7.07	7.554	6.467	4.544
7.25	7.552	6.466	4.544
8.00	7.534	6.462	4.539
8.37	7.513	6.453	4.532
8.64	7.467	6.435	4.517
8.96	7.436	6.432	4.518
9.05	7.405	6.419	4.508
9.10	7.386	6.416	4.507
9.38	7.331	6.393	4.488
10.04	7.211	6.356	4.463
10.10	7.202	6.355	4.464
10.70	7.154	6.338	4.450
11.02	7.147	6.336	4.448
12.05	7.152	6.337	4.434
12.30	7.168	6.342	4.421
12.40	7.200	6.355	4.403
12.86	7.221	6.355	4.374
13.02	7.270	6.374	4.346
13.20	7.270	6.349	4.273
13.30	7.265	6.345	4.268

Figure S5. Superimposition of 2D ^{1}H-^{13}C spectra for the free P1 ligand at different pH values. In the inset a plot of the relative ^{13}C chemical shift variation $\Delta\delta = \delta_{pHi} - \delta_{pH0}$ for C6 (●), C3 (■) and C7 (▲); pH_0=1.67 (red), and pH_i=5.7 (orange), 8.2 (green) and 12.4 (blue), respectively.

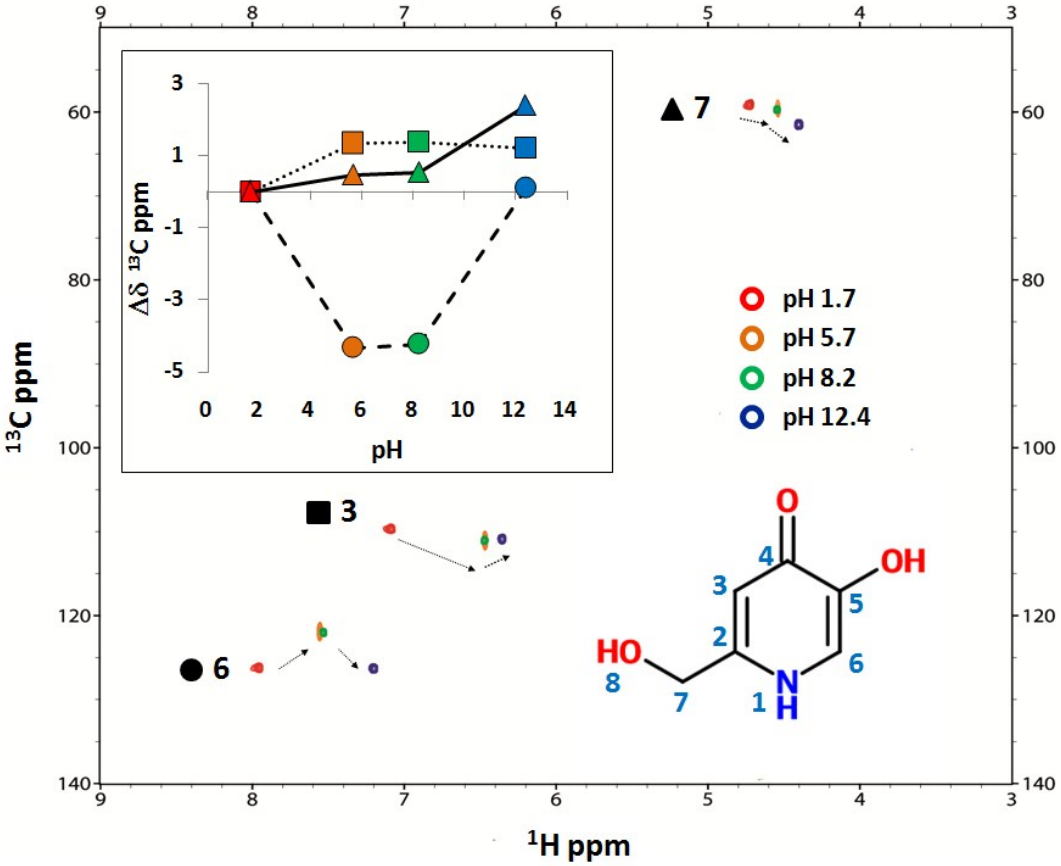

Figure S6. Stacked aromatic region of 1D ^{1}H NMR spectra of the P1 ligand by increasing of substoichiometric amounts of Fe^{3+} ion, in phosphate buffer solution (pH = 7) at 298 K. In the inset, the relative ratio of H3/H6 in term of peak integral (black rhombus) and peak height (orange square).

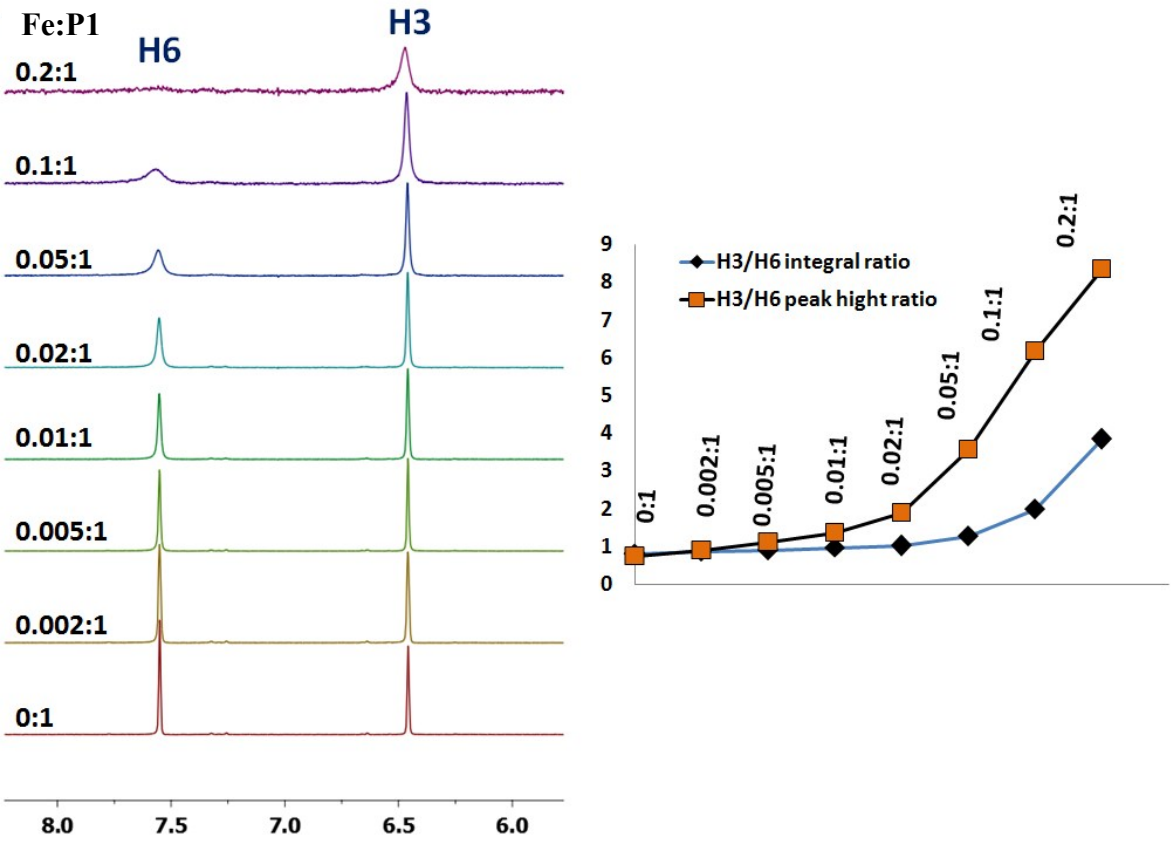

Figure S7. Stacked 1D ^{1}H NMR spectra of P1 ligand by increasing amount of Ga^{3+}, as a diamagnetic probe of Fe^{3+}, in phosphate buffer solution at 298 K.

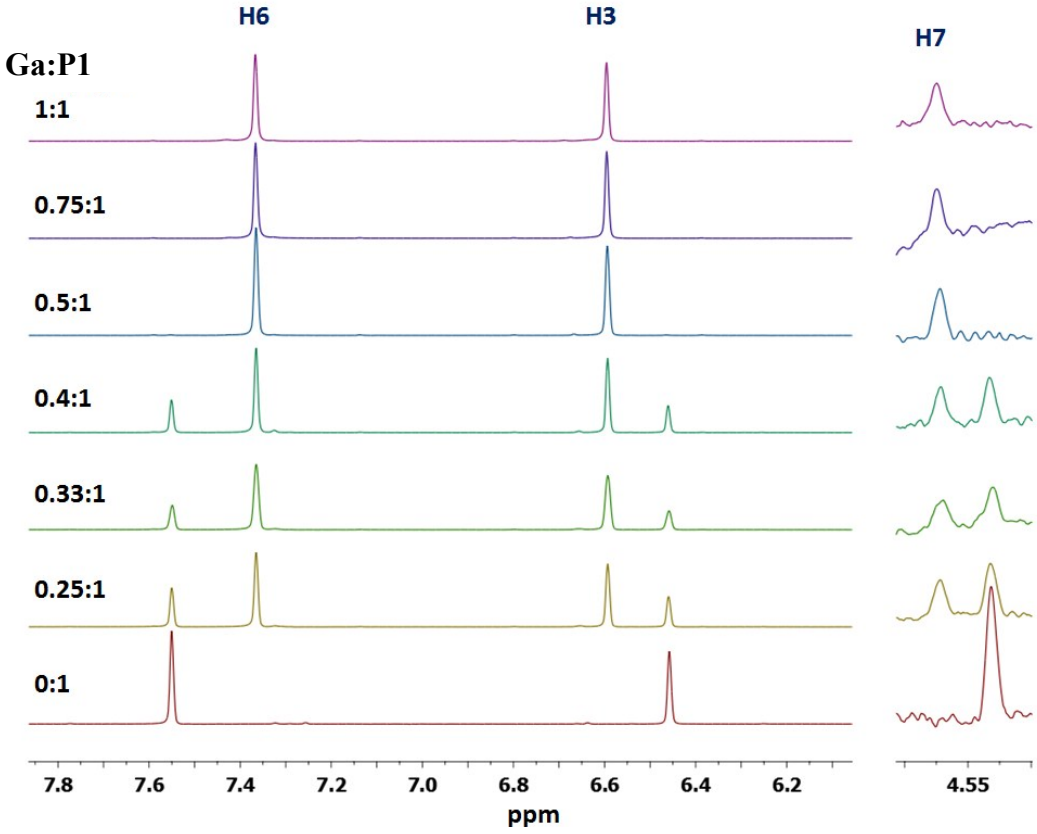

Figure S8. The comparison of the relative ratio of H3/H6 in term of peak integral and peak high ratio between pH 7 (black square) and pH 11.5 (orange rhombus).

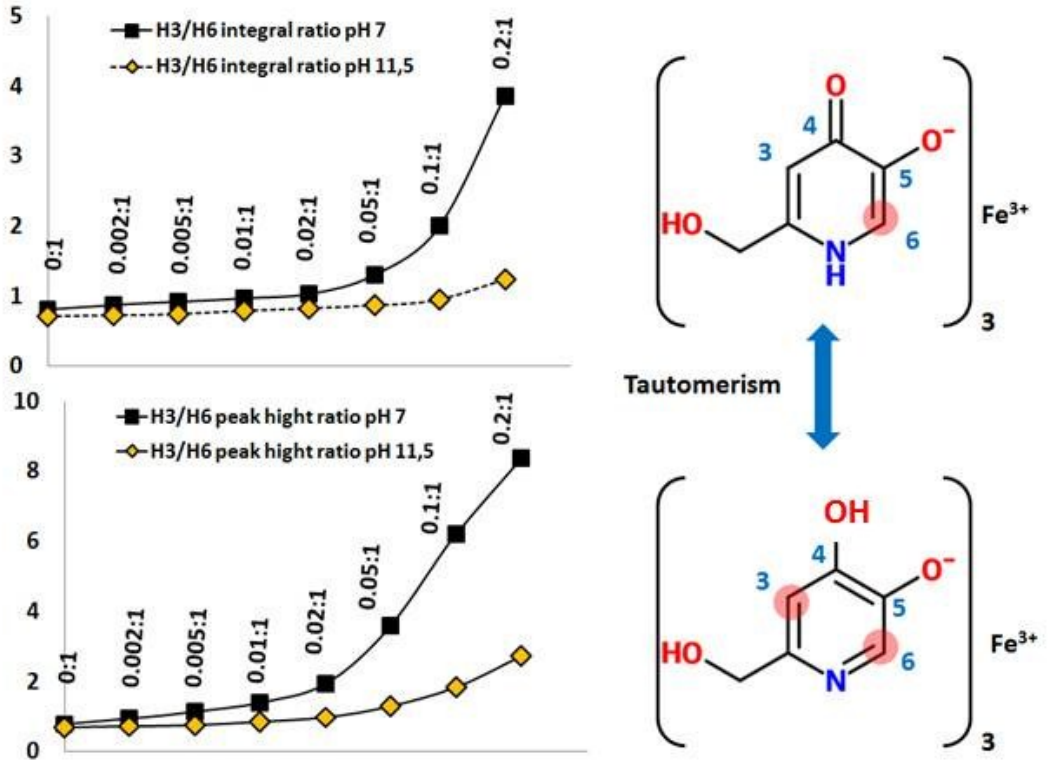

Figure S9. Experimental data for peaks of the P1 ligand at pD 7 in D_2O solution are shown at the top of the panel and compared with the data calculated for the $[C_6H_8O_3N]^+$ (142.061 m/z, Panel A) $[C_6H_7DO_3N]^+$ (143.057 m/z, Panel B), $[C_6H_6D_2O_3N]^+$ (144.063 *m/z,* Panel C), $[C_6H_5D_3O_3N]^+$ (145.070 *m/z*, Panel D) and $[C_6H_4D_4O_3N]^+$ (146.076 *m/z* Panel E).

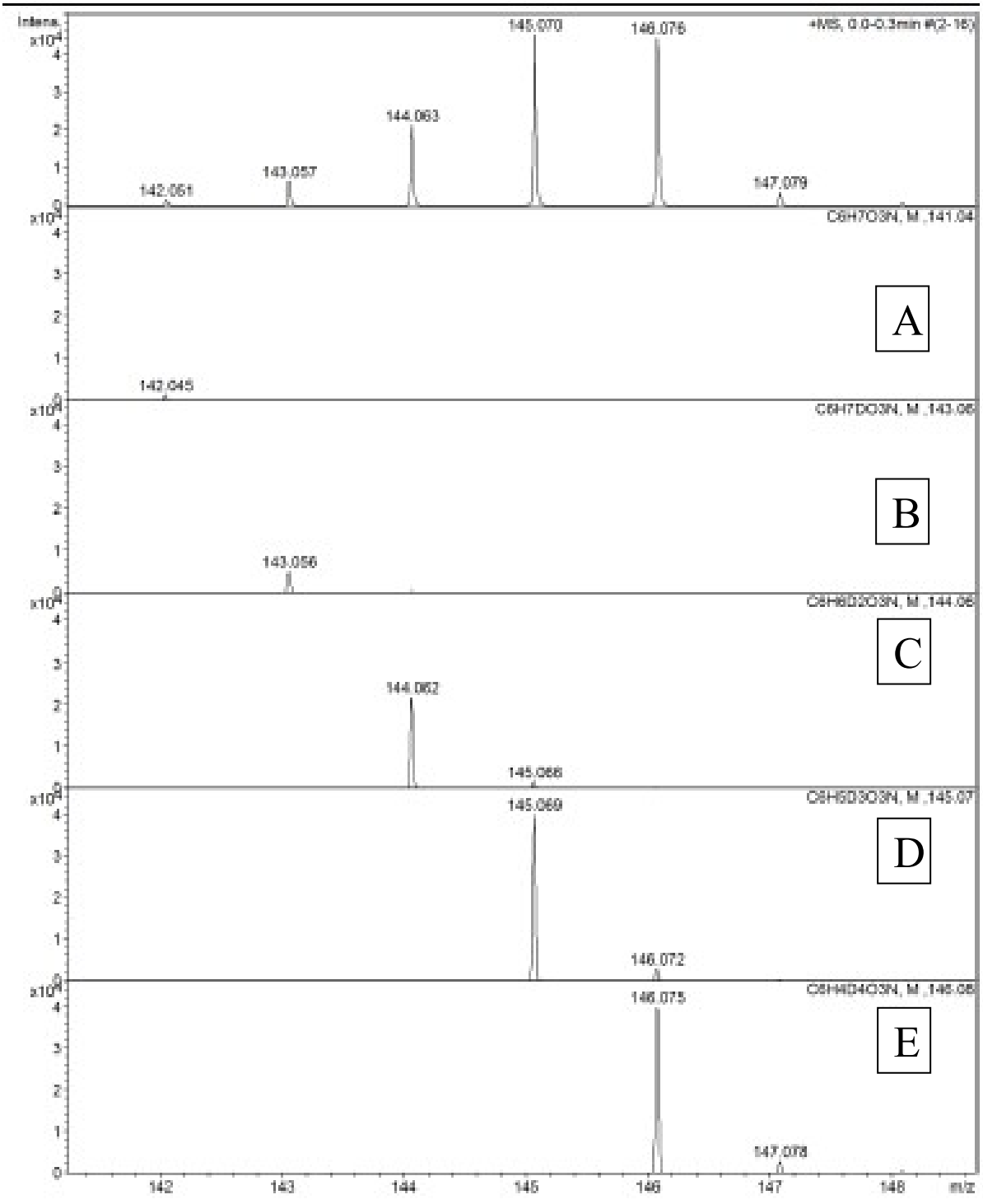

Table S28. ESI-MS *m/z* data of **P1** in aqueous solution at different pH.

pH	Negative	Intensity	Positive	Intensity
1.68	140.032	10000	142.054	15000
6.13	140.034	8000	142.054	8000
11.5	139.032	2500	-	-
13.7	139.033	4000	-	-

Figure S10. Fe^{3+}–P1 complexes. Experimental data for peak *m/z* = 333.998 (Panel A), 336.004 (Panel B), 409.940 (Panel C), 499.029 (Panel D) and 515.010 (Panel E) are shown at the top of the panel and compared with the data calculated for the Fe^{3+} complex (lower panel).

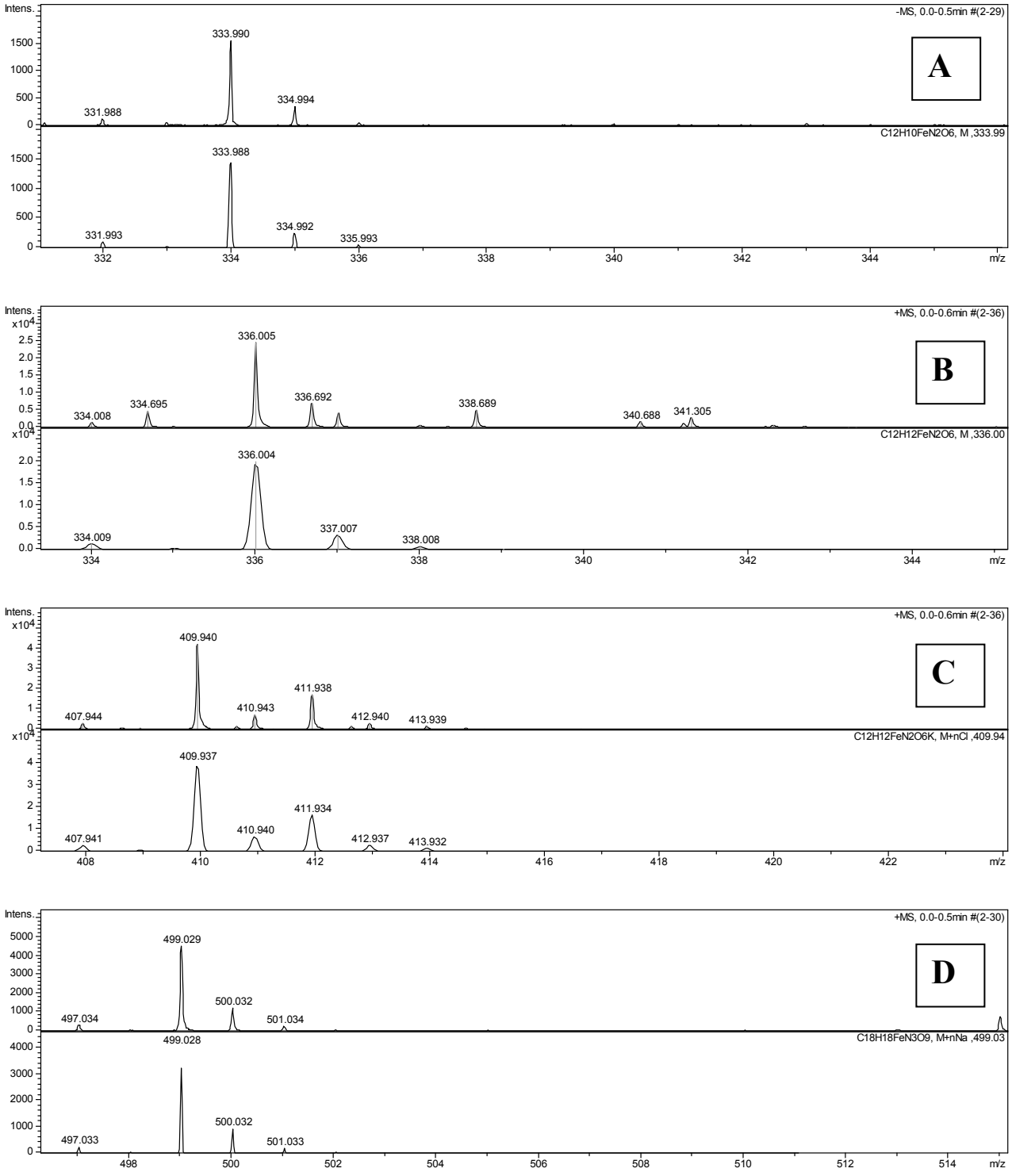

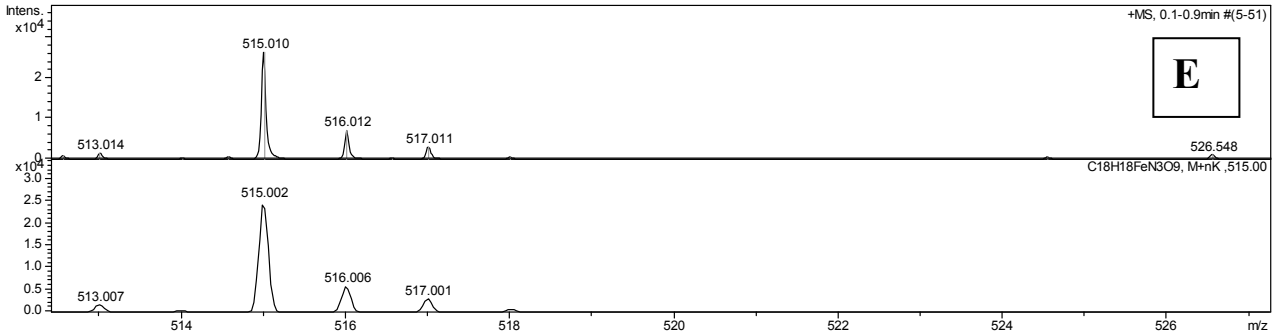
Intens.
x10^4
+MS, 0.1-0.9min #(5-51)
515.010
516.012
517.011
513.014
526.548
E
C18H18FeN3O9, M+nK ,515.00
515.002
516.006
517.001
513.007
514
516
518
520
522
524
526
m/z

Table S29. ESI-MS *m/z* data of Fe^{3+}–P1 aqueous solution in different pH.

pH	Negative	Intensity	Positive	Intensity	Species
2.16	-	-	336.004	15000	$[FeL_2H_2]^+$
			409.944	25000	$[FeL_2H_2+Cl+K]^+$
			515.002	800	$[FeL_3H_3+K]^+$
3.25	-	-	336.005	20000	$[FeL_2H_2]^+$
			409.940	40000	$[FeL_2H_2+Cl+K]^+$
			515.006	2500	$[FeL_3H_3+K]^+$
6.78	-	-	515.015	25000	$[FeL_3H_3+K]^+$
9.52	-	-	515.005	15000	$[FeL_3H_3+K]^+$
11.10	-	-	515.008	12000	$[FeL_3H_3+K]^+$
>11	333.998	1500	-	-	$[FeL_2]^-$
	-	-	336.001	5000	$[FeL_2H_2]^+$
	-	-	499.029	4000	$[FeL_3H_3+Na]^+$
	-	-	515.002	800	$[FeL_3H_3+K]^+$

Figure S11. Al^{3+}–P1 complexes. Experimental data for peak *m/z* = 305.030 (Panel A), 307.056 (Panel B), 448.101 (Panel C), 470.074 (Panel D) and 486.048 (Panel E) are shown at the top of the panel and compared with the data calculated for the Al^{3+} complex (lower panel).

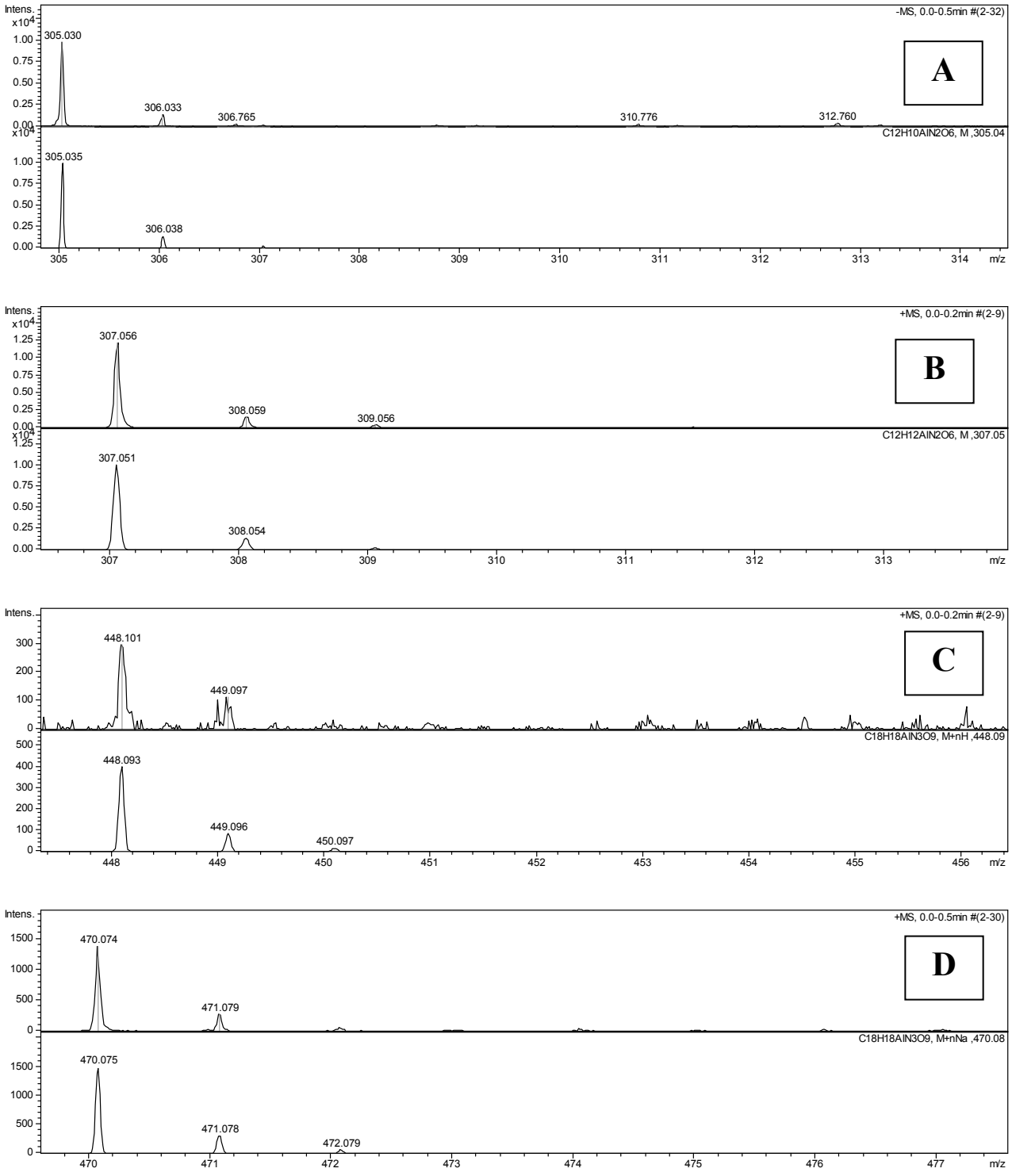

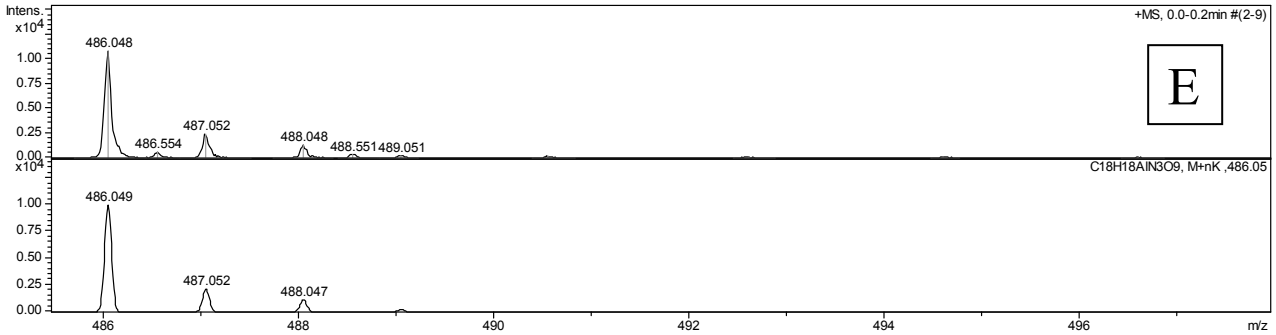
Intens.
x10^4
1.00
0.75
0.50
0.25
0.00
486.048
486.554
487.052
488.048
488.551
489.051
+MS, 0.0-0.2min #(2-9)
E
C18H18AlN3O9, M+nK ,486.05
486.049
487.052
488.047
486
488
490
492
494
496
m/z

Table S30. ESI-MS *m/z* data of Al^{3+}–P1 aqueous solution at different pH.

pH	Negative	Intensity	Positive	Intensity	Species
4.06	305.032	3000	-	-	$[AlL_2]^-$
6.21	305.032	5000	-	-	$[AlL_2]^-$
	-	-	486.049	25000	$[AlL_3H_3+K]^+$
7.00	305.032	300	-	-	$[AlL_2]^-$
	-	-	307.051	15000	$[AlL_2H_2]^+$
	-	-	448.101	300	$[AlL_3H_3+H]^+$
7.70	-	-	486.049	20000	$[AlL_3H_3+K]^+$
10.83	305.032	10000	-	-	$[AlL_2]^-$
	-	-	486.049	25000	$[AlL_3H_3+K]^+$
>11	305.043	300	-	-	$[AlL_2]^-$
	-	-	307.049	1500	$[AlL_2H_2]^+$
	-	-	470.074	1250	$[AlL_3H_3+Na]^+$

Figure S12. Cu^{2+}–P1 complexes. Experimental data for peak *m/z* = 236.924 (Panel A), 341.989 (Panel B), 344.009 (Panel C), 365.985 (Panel D) and 381.963 (Panel E) are shown at the top of the panel and compared with the data calculated for the Cu^{2+} complex (lower panel).

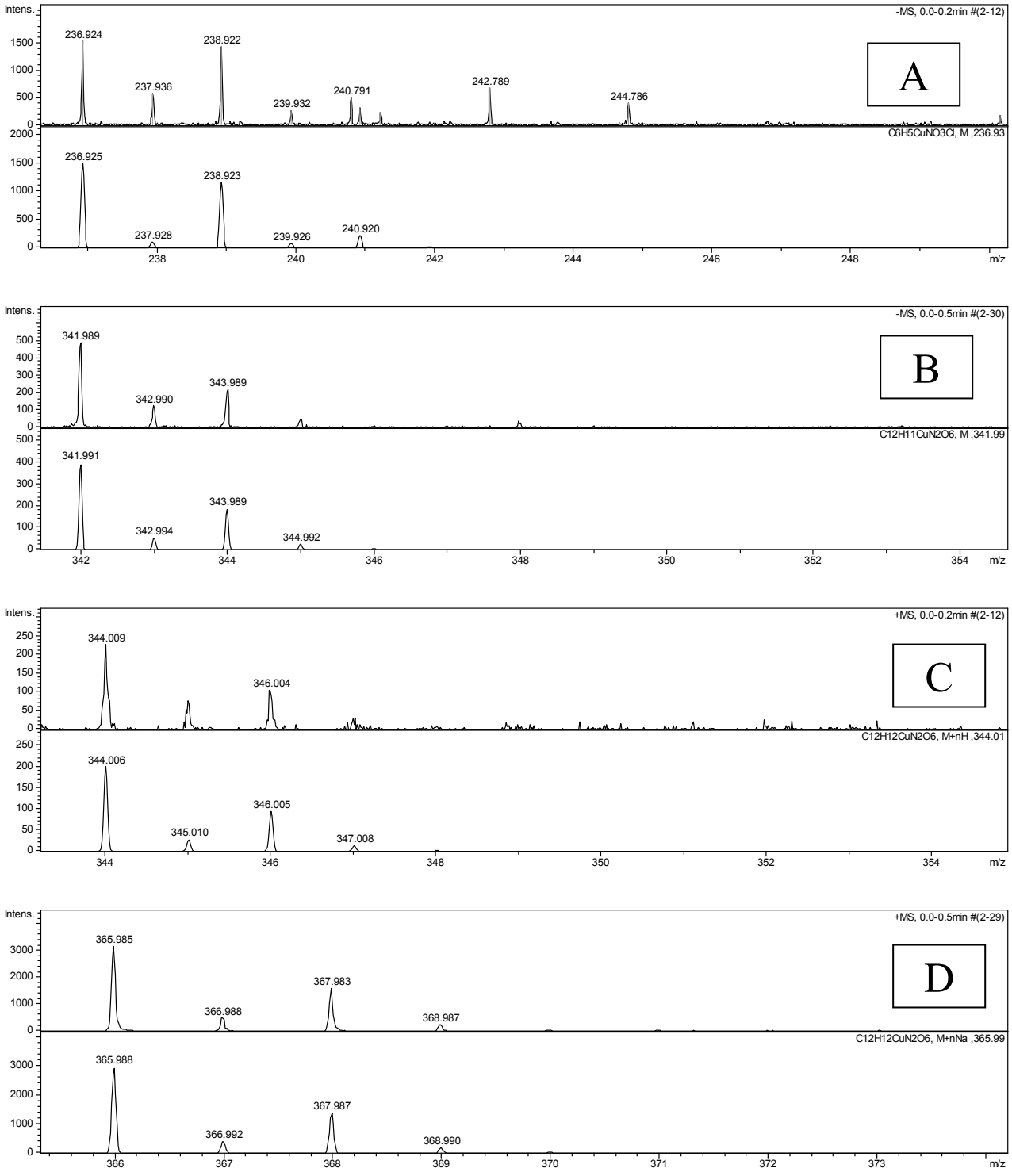

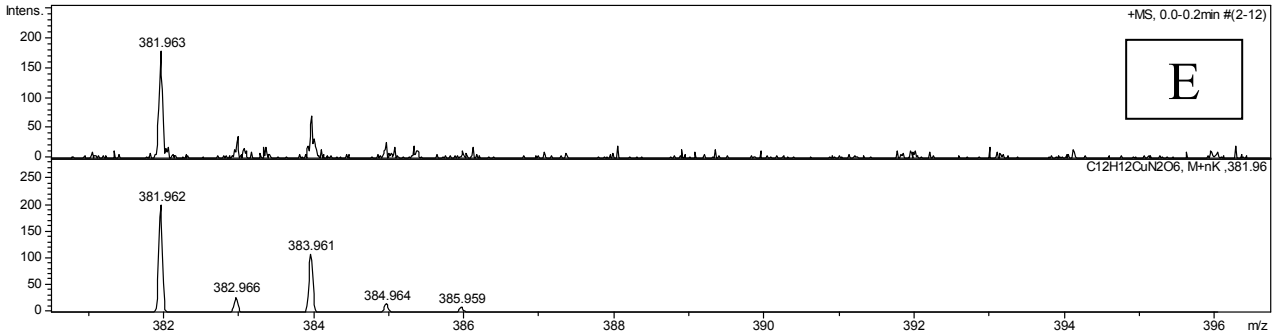
Intens.
+MS, 0.0-0.2min #(2-12)
381.963
E
C12H12CuN2O6, M+nK ,381.96
381.962
383.961
382.966
384.964
385.959
m/z

Table S31. ESI-MS *m/z* data of Cu^{2+}–P1 aqueous solution at different pH.

pH	Negative	Intensity	Positive	Intensity	Species
3.90	236.924	1500	-	-	$[CuL+Cl]^-$
7.00	-	-	344.009	200	$[CuL_2H_2+H]^+$
	-	-	381.963	200	$[CuL_2H_2+K]^+$
>11	341.989	500	-	-	$[CuL_2H]^-$
	-	-	344.002	2000	$[CuL_2H_2+H]^+$
	-	-	365.985	2000	$[CuL_2H_2+Na]^+$

Figure S13. Zn^{2+}–P1 complexes. Experimental data (pH 7.0) for peak *m/z* = 382.970 are shown at the top of the panel and compared with the data calculated for the zinc(II) complex (lower panel).

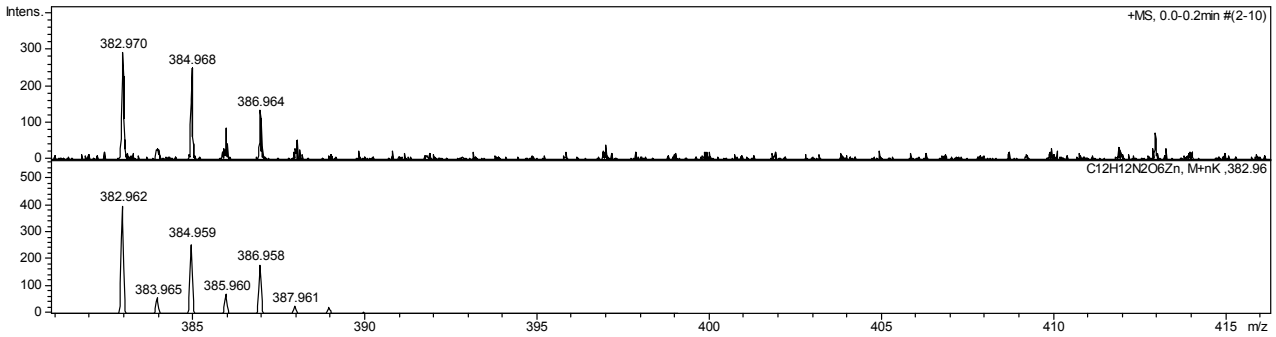

Table S32. Complex formation constants (log β) of P1 with Fe^{3+}, Al^{3+}, Cu^{2+} and Zn^{2+} ions, and literature complex formation constants of DFP and 3,4-hopo. The charges are omitted for simplicity.

	P1					**DFP**				**3,4-hopo**			
Model	**Fe^{3+}**	**Al^{3+}**	**Cu^{2+}**	**Zn^{2+}**	**Model**	**Fe^{3+}** [1]	**Al^{3+}** [2]	**Cu^{2+}** [1]	**Zn^{2+}** [3]	**Fe^{3+}** [4]	**Al^{3+}**	**Cu^{2+}** [5]	**Zn^{2+}** [5]
ML	25.92(9)	23.32(9)	21.78(7)	18.79(6)	ML	15.01(1)	11.91	10.42	7.24	14.26(3)	----	9.49	6.81
ML_2H_2	49.12(1)	45.18(6)	41.42(7)	36.70(4)	ML_2H	----	----	21.98		----	----	----	----
ML_2H	----	----	34.21(5)	26.02(9)	ML_2	27.03(1)	22.83	19.09	13.55	25.73(1)	----	17.13	12.54
ML_2	----	----	24.68(5)	----	ML_2H_{-1}	----	----	8.49	2.30	----	----	----	----
ML_3H_3	71.43(6)	65.25(7)	----	----	ML_3	37.43(1)	32.25	----	15.2	34.91(1)	----	----	----
ML_3H_2	65.33(3)	58.30(4)	----	----									
ML_3H	55.62(9)	47.48(5)	----	----									
ML_3	44.63(5)	38.41(5)	----	----									
pM^{n+}	22.0	15.1	10.1	6.3	pM^{n+}	20.7	15.4	10.1	6.2	20.6	NF	9.7	6.4

[1] V. M. Nurchi, G. Crisponi, T. Pivetta, M. Donatoni and M. Remelli, *Journal of Inorganic Biochemistry*, 2008, **102**, 684-692.

[2] D. J. Clevette, W. O. Nelson, A. Nordin, C. Orvig and S. Sjoeberg, *Inorganic Chemistry*, 1989, **28**, 2079-2081.

[3] T. Jakusch, K. Gaida-Schrantz, Y. Adachi, H. Sakurai, T. Kiss, L. Horvath, *J. Inorg. Biochem*., (2006), 100:1521-1526.

[4] R. C. Scarrow, P. E. Riley, K. Abu-Dari, D. L. White and K. N. Raymond, *Inorganic Chemistry*, 1985, **24**, 954-967.

[5] H. Stunzi, L. Harris, D. Perrin and T. Teitei, *Australian Journal of Chemistry*, 1980, **33**, 2207-2220.